

P. Kiedron
518 437 8737
kiedron@asrc.cestm.albany.edu

17 November, 2003

RSS Performance Evaluation During First Six Months Since Its Deployment

1. Summary and Conclusions

RSS was deployed at SGP in May 2003. It operated semi-continuously for over 180 days with approximately 10% downtime. SGP staff was trained to perform radiometric calibrations with (a) Portable Calibrator (see the picture) when RSS is in vertical position and (b) Licor when RSS is in horizontal position and to perform wavelength calibration with Oriel's HgCd lamp both in horizontal and vertical positions.



Erik Yager of ASRC demonstrates calibration with Portable Calibrator in May 2003 at SGP

Between May and November 2003 11 calibrations with Portable Calibrator and four with Licor and four HgCd calibrations were performed. From this data we estimated responsivity drift. The results are only partially corroborated by the results from 45 recorded Langley events. The wavelength stability was determined from HgCd measurements and from solar measurements via correlation with Fraunhofer spectral features. The latter allowed as to measure wavelength shifts in every spectrum.

1.1 Responsivity drift

Average responsivity dropped 15% during the first 70 days of operation (see red curve in Figure 1). After 60 days of operation a wavelength dependent periodic features resembling an etaloning effect started to develop (see blue curve in Figure 1). Within subsequent 40 days the depth of the modulation of this feature reached $\pm 7\%$. In the last sixty days of operation the rate of change of responsivity significantly decreased.

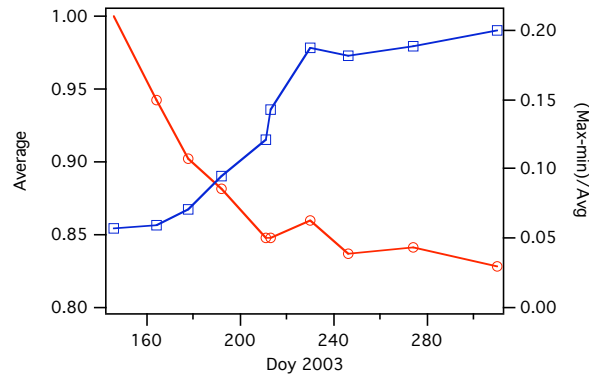


Figure 1. Relative change of responsivity with time (red-change of average, blue-change of amplitude of the periodic feature).

By analyzing direct beam spectra (on clear sky days) we could conclude that the periodic component of the responsivity remains stable within each day. Thus we have some degree of confidence that we can salvage data from this rather unstable instrument and obtain radiometrically calibrated spectra. We derive responsivity for each day by interpolating responsivities from 11 measurements. The final validity of this approach will be verified when data from Aerosol IOP in May 2003 and Diffuse IOP in October 2003 will be compared with MFRSR data and modeled irradiances.

1.2 Wavelength stability

During the first 50 days wavelength was stable to within ± 0.2 pixel (see Figure 2).

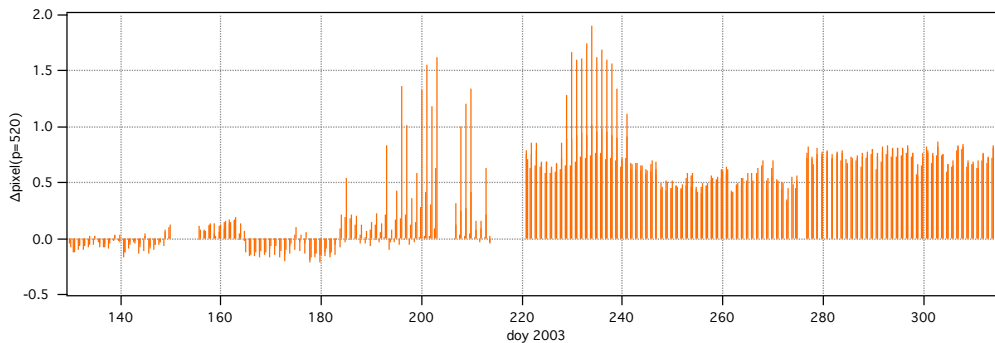


Figure 2. Wavelength shifts (in pixels) calculated from individual solar spectra. The results are from three spectra (morning, noon and afternoon) per day.

However in July and August when external temperature exceeded 35°C the thermal stabilization of RSS was lost resulting in wavelength shifts of up to +2 pixels. (These are relatively large shifts as fwhm is only 2.5 pixel.) In the beginning of August the spectrum position on the CCD shifted by 0.5-0.6 pixel to a new equilibrium. And again after brief down time in September the equilibrium seemed to shift by +0.25 pixel

The wavelength instability complicates data processing of individual spectra. It is fortunate that we can detect the wavelength shifts. However the algorithm is relatively complicated and has a long running time. Nevertheless we will have to implement it to obtain precise absorption bands locations and to correct inputs for Langley regressions. Also the wavelength shifts have impact on radiometric accuracy. For instance ± 1 pixel shifts result in $\pm 1.5\%$ for wavelengths less than 900nm and in $\pm 2.5\%$ at 1000nm (see Figure 3).

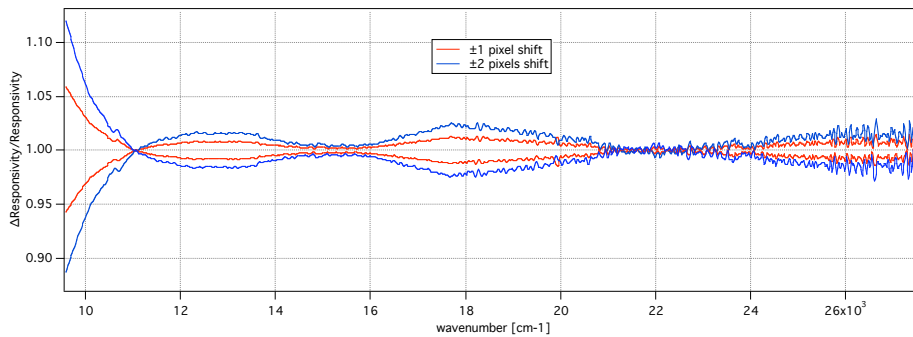


Figure 3. Radiometric error due to ± 1 and ± 2 pixel shifts.

1.3 Data availability

For the first six months of operation our data processing package (RSStk) was using only one fixed responsivity that remained valid for only 2 weeks at best.

Currently the data are being reprocessed with time dependent responsivity and wavelength shift correction. We did not implement wavelength correction to each individual spectrum. It is applied only once a day. Thus the results, particularly for hot days of Summer 2003, may contain relatively large wavelength errors. In Figure 4 we show six spectra with the original uncorrected calibration and after all corrections were applied.

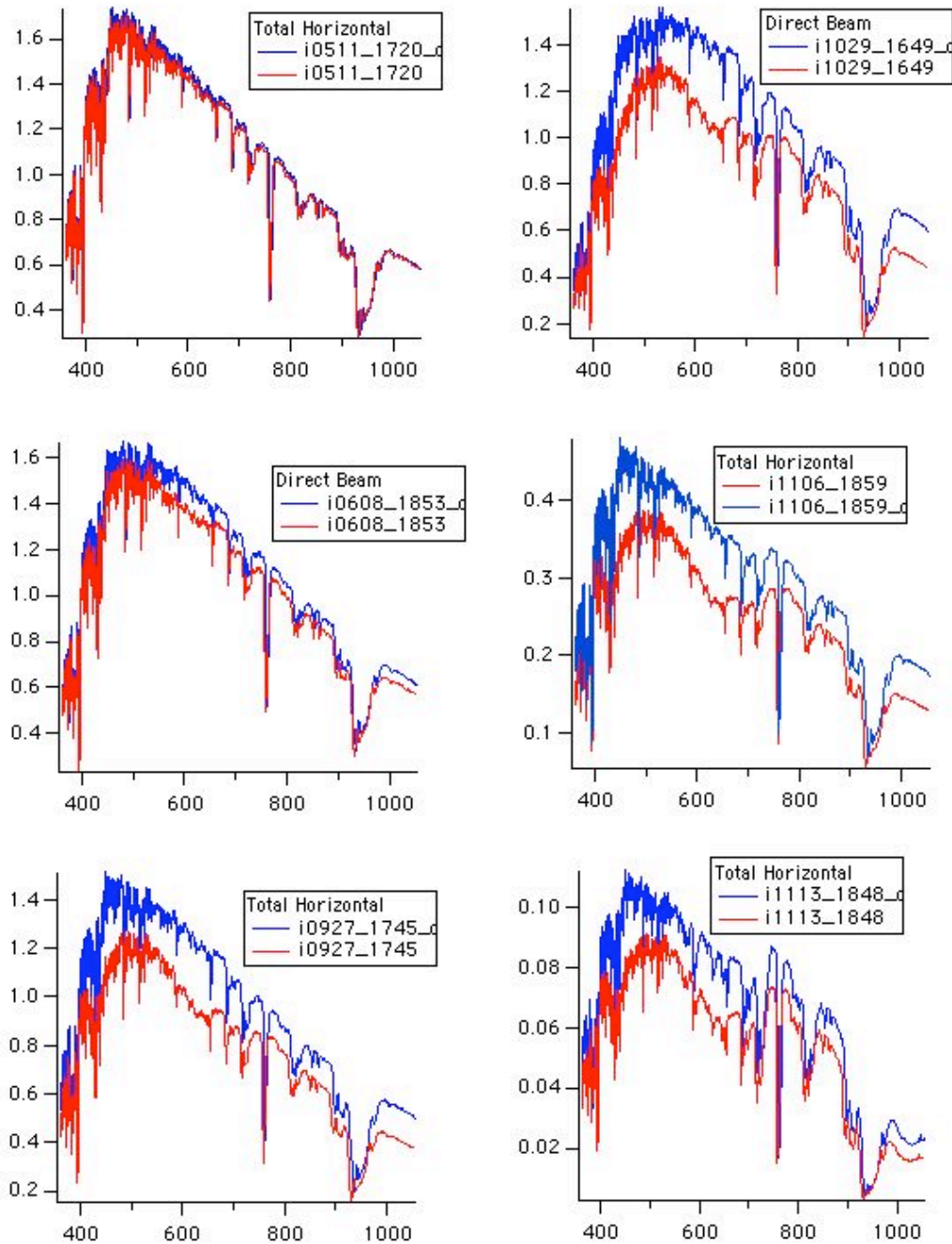


Figure 4. Spectra with uncorrected (red) and corrected (blue) calibrations

1.4 Modes of failure

Apart from power shortages at SGP that account for majority of 10% failure rate we have identified several modes of failure that can be traced to RSS's integral linux computer, the so-called "linux box" also referred to as "core CPU" by YES, Inc. The following list was prepared by Jim Schlemmer of ASRC:

(i) Upon installation, we changed the instrument ID and name to fall in line with our previous RSS instruments. This apparently caused the instrument to stop working. Although these parameters are fully configurable via the YESDAQ GUI, we were told not to mess around with them "capriciously", as this caused the system to become unstable. We also changed the GUI admin password and were informed that because we had a semi-colon in the password, the system became unusable.

(ii) The system has occasionally stopped working at the RSS instrument level. This is an unresolved issue (could be in firmware or software) and involved the controlling program (the one that talks directly to the instrument) being unable to get the instrument going after multiple attempts. In each instance, the controlling program quietly gave up and no data was taken until somebody or some external program noticed.

(iii) The system keeps its raw data in both SQL form and as plain, hourly text files. We have seen problems whereby the text files have mysteriously dried up even as the mysql server and the RSS itself continued to operate.

(iv) The unexplained gaps in the hourly text files prompted us to switch over to direct SQL queries for raw data retrievals. Recently, however, we have witnessed the mysql server hanging on the RSS internal linux machine. The web pages and RSS seemed to be functioning properly but the data was not being added to the SQL database. In this case, the mysql server started behaving normally again after a couple of days. Whether or not the silent hand of Yankee was at work, we do not yet know.

(vi) The instrument failed to recognize the end of calibration and continued to dump solar scans into the calibration file for a whole day until we discovered the problem and restarted the instrument. This problem most likely originated in the linux box software.

(vii) On one occasion after being alerted by Mike Rainwater of SGP that the shadowing is imperfect we found that restarting the instrument fixed the problem. This would imply a time error in the ephemeris algorithm. In the current configuration we cannot verify time accuracy in real time. The instrument has to be stopped via the web interface.

1.5 Conclusions

(i) The radiometric stability of RSS is significantly worse than the stability of the previous two RSS prototypes. We think that the schedule of two calibrations per month needs to be continued to be able to correct the responsivity drift. When (and if) the rate of change of responsivity tapers off the frequency of calibrations would be reduced.

(ii) The wavelength stability is not better than the stability in the prototype RSS's that had significantly less sophisticated mechanical design and temperature control. However we think that at SGP location the current wavelength stability is sufficiently good for ten out of twelve months. When external temperature exceeds 35°C additional signal processing is necessary to correct wavelength shift errors. We do not think that this problem needs to be solved at this time by RSS manufacturer.

(iii) The current configuration relies on the RSS integral “linux box” with its software (by YES, Inc.). The “linux box” has a serial connection with the RSS-micro board and its firmware (by ASRC). The communication via the “linux box” is cumbersome and inflexible from our point of view. At the same time the expected benefits of the linux box and the web interface it supports are not important in our application.

Appendix I: More on radiometric stability

In Figure 5 ratio of responsivities is depicted. Results presented in Figure 1 were derived from Figure 5. And in Figure 6 we plotted responsivity change as function of time for four wavelengths and compared them with Vo's from Langley regressions. There were 45 Langley events during this time.

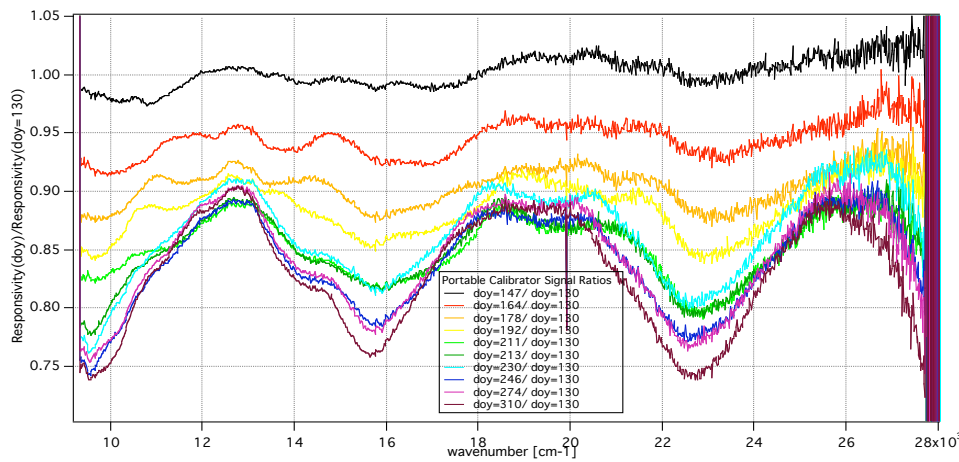


Figure 5. Ratio of responsivities derived from 11 measurements with Portable Calibrator.

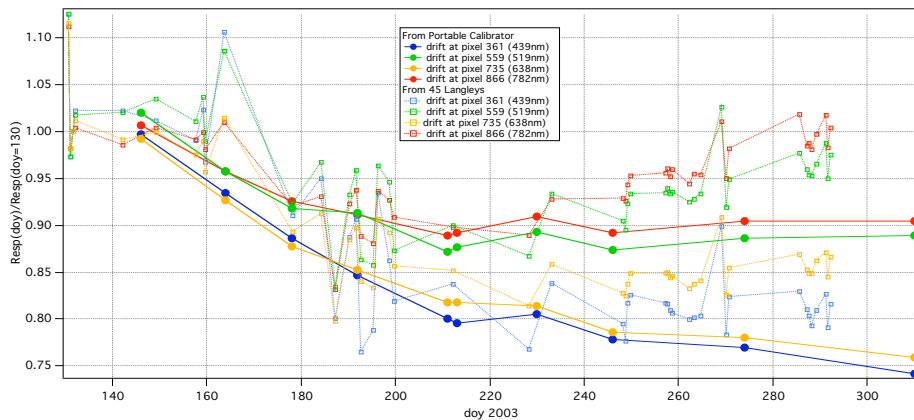


Figure 6. Drift comparison as derived from Portable Calibrators and 45 Langley events at three wavelengths.

For days 240-300 Vo's diverge significantly from Portable Calibrator readings. We cannot explain this discrepancy. We decided to trust Portable Calibrators for two reasons: (1) Portable Calibrator measurements are congruent to within $\pm 2\%$ with Licor

measurements (see Figure 7) and (2) for large responsivity changes $\Delta R/R$ the frequency of Langley events is too small and individual Langley results are biased with errors larger than $\Delta R/R$ in cases of unstable atmosphere.

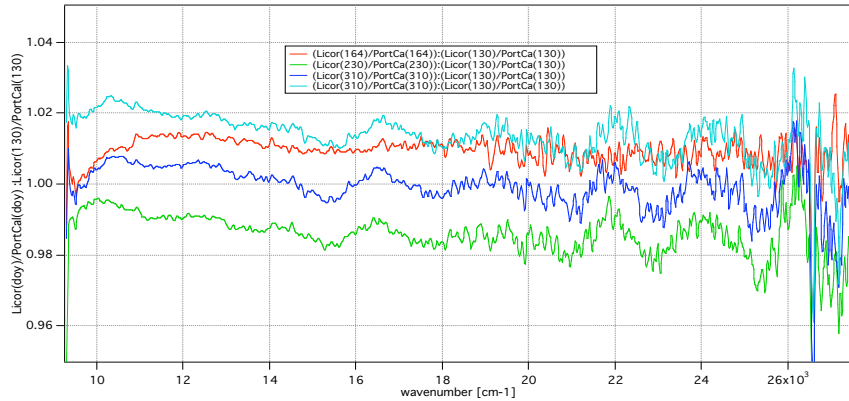


Figure 7. Ratio of responsivities derived from Licor to those derived from Portable Calibrator

The curves in Figure 5 strongly suggest existence of absorption and etaloning effect. We do not know whether the two effects are related. The etaloning effect has almost a constant frequency. This frequency is equivalent to 780nm optical thickness of the etalon. We do not see the evidence that the etalon thickness was increasing from 0 to 760nm, i.e., there is no intermediate frequency. Thus the etalon was created in relatively short time. The increasing depth of modulation implies that either the reflectivity of one interface of the etalon is increasing or the effective reflectivity is increasing. The latter would be the case if etalon had area that increases from 0% of the beam's cross section to 100% of the beam's cross section. This scenario could be imagined as an air bubble between, say, two epoxied filters, that grows in a diameter.

The following equation for transmittance of an etalon is used to demonstrate

$$T = a \left[b \left(1 - \left(1 - \frac{A}{1-R} \right)^2 \frac{1}{1 + F \sin^2 \frac{\varphi}{2}} \right) \right]$$

the feasibility of this scenario. In the equation

$$F = \frac{4R}{(1-R)^2}$$

where R is interface reflectivity and the phase

$$\varphi = \frac{4n}{\lambda} nh \cos \theta + 2\theta$$

where nh is optical thickness of etalon, θ is angle of refraction in etalon and θ is phase change during internal reflection on etalon interface and A is absorption in etalon, b ratio of etalon area to beam area and a is transmittance outside of etalon.

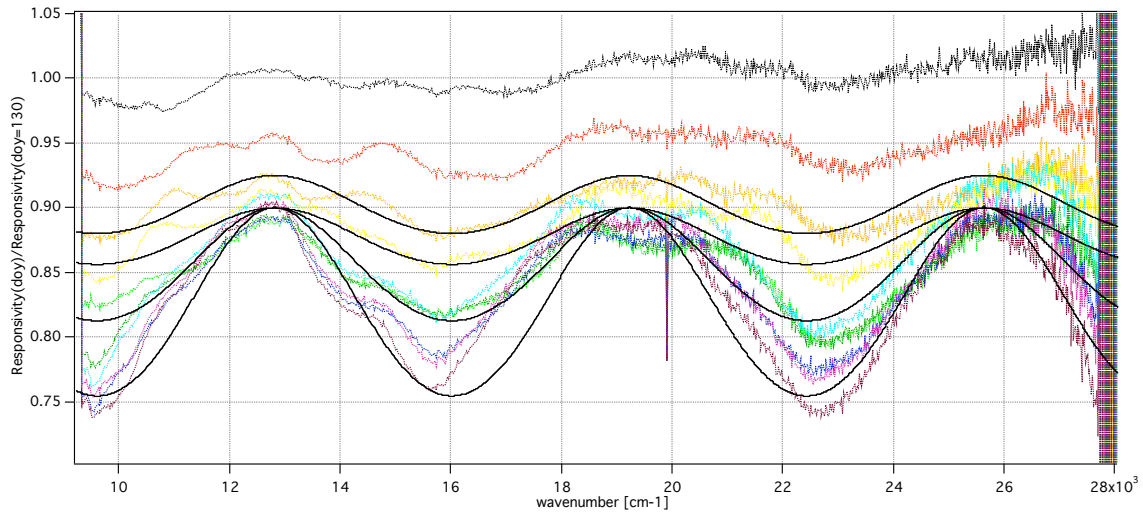


Figure 8. Ratio of responsivities derived from 11 measurements with Portable Calibrator and several calculated transmittances of an etalon.

In Figure 8 four calculated transmittance curves were appended to Figure 5. The curves were calculated for the following parameters:

<i>a</i>	<i>b</i>	<i>A</i>	<i>R</i>	\square	\square	<i>nh [nm]</i>
0.900	1.00	0	0.044	0	0	780
0.900	0.600	0	0.044	0	0	780
0.900	0.300	0	0.044	0	0	780
0.925	0.300	0	0.044	0	0	780

Appendix II: More on wavelength stability

In Figure 1 wavelength shifts $\Delta p(p=520)$ in the vicinity of pixel=520 are depicted. The pixel shifts, however, are slightly wavelength dependent. So in addition to an offset a multiplicative factor need to be introduced. This factor is proportional to the increment of the pixel shift, for instance to $\Delta\Delta p = \Delta p(\text{pixel}=1039) - \Delta p(p=0)$.

In Figure 9 $\Delta\Delta p$ is plotted against Δp . We clearly can see two epochs: once when $\Delta p=0$ and once when $\Delta p=0.6$. Respectively $\Delta\Delta p=0.15$ and $\Delta\Delta p=0.25$. Also when Δp increases then $\Delta\Delta p$ decreases.

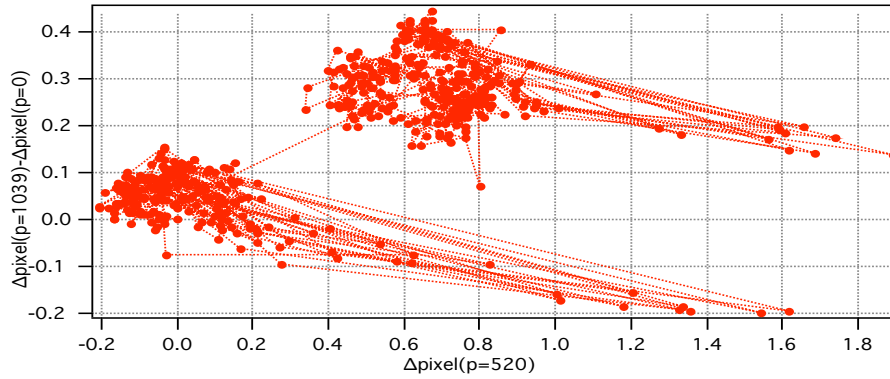


Figure 9. Pixel shift increment $\Delta p(\text{pixel}=1039)-\Delta p(p=0)$ versus pixel shift $\Delta p(p=520)$

Temperature of the casting suppose to be held at 45°C and the temperature of the prism block at 49°C. Figures 10 and 11 show that when external temperature exceeds 32°C casting temperature control begins to go out of lock.

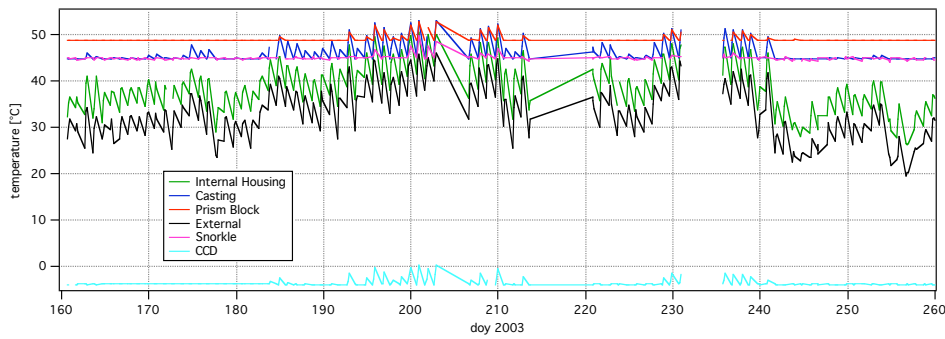


Figure 10. Temperatures versus time

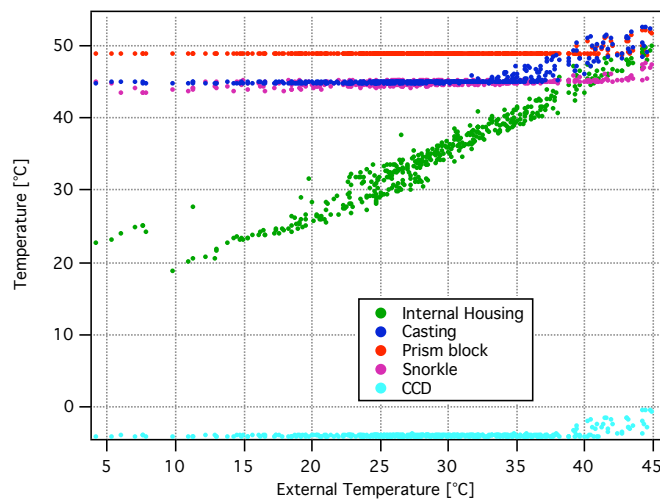


Figure 11. Temperatures versus external temperature

When the external temperature exceeds 39°C the prism block temperature begins to go out of lock. Also the temperature of CCD goes out lock at the same time.

The blue and red panels of Figure 12 suggest the mechanism of wavelength shifts for temperatures larger than 32°C. Thus when the casting temperature is between 45°C and 49°C the wavelength shift, most likely due to geometry changes caused by thermal expansion, occurs. But when the casting temperature exceeds 49°C then also the prism block temperature increases resulting in index of refraction change. This explains the change of slope at t=49°C in the blue panel of Figure 12.

For temperatures lower than 32°C there is a very weak correlation of wavelength shifts with the external temperature and the internal housing temperature. However we this does not accounts for shifts of ± 0.2 pixel.

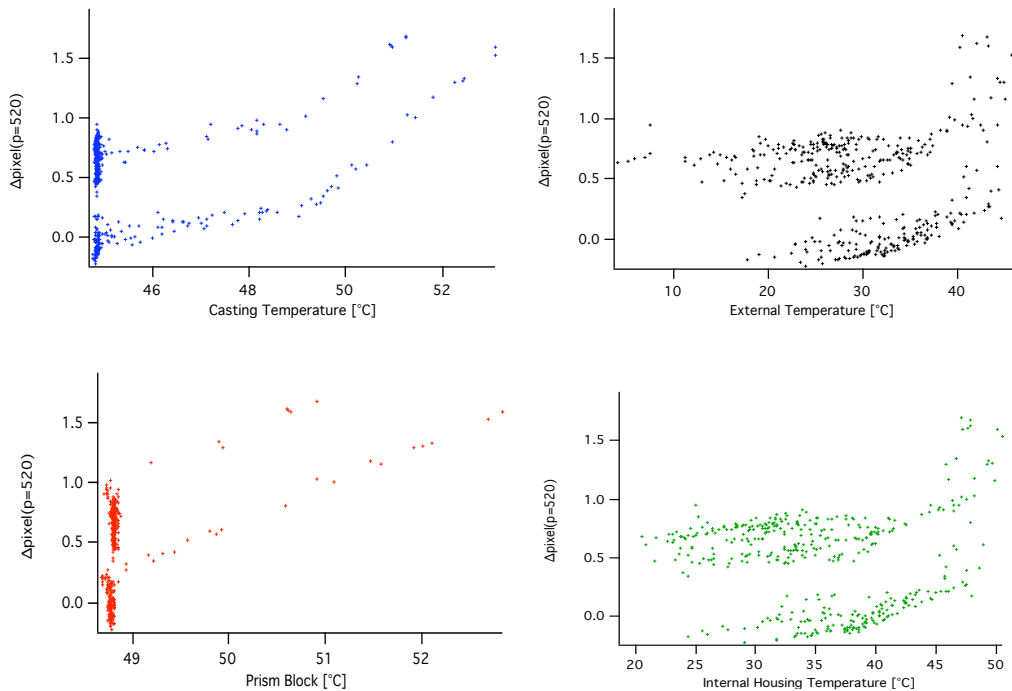


Figure 12. Wavelength shift versus four temperatures